Theoretical and Applied Climatology (2020) 139:447–459
https://doi.org/10.1007/s00704-019-02978-7

ORIGINAL PAPER

A spatiotemporal analysis of Indian warming target using CORDEX-SA experiment data

Deepak Kumar Prajapat[1] · Jyoti Lodha[1] · Mahender Choudhary[1]

Received: 20 June 2019 / Accepted: 14 August 2019 / Published online: 30 August 2019

Abstract

It is important to estimate a high-resolution spatiotemporal distribution of temperature rise under climate change for effective adaptation and mitigation planning. This paper studies the threshold crossing time (TCT) for eight Indian warming targets (IWTs) between 1.5 and 5 °C based on regional climate models (RCMs) participating in The Coordinated Regional Downscaling Experiment (CORDEX)—South Asia project. To evaluate the performance of CORDEX experiments in simulating the near-surface mean temperature, the model performance index (MPI) is used which represents that the CanESM experiment performs best for simulating T_{mean} over India. All India average T_{mean} projected by the multi-model ensemble (MME) represents that 1.5 °C TCT is about 2033 ± 3 and 2028 ± 3 in RCP4.5 and RCP8.5 scenarios, respectively. During the twenty-first century, Indian subcontinent can experience five IWTs (1.5–3.5 °C) under RCP4.5 and all eight under scenario RCP8.5. The fastest warming region in India is the western Himalayan region (North India) and north-west region (Indian Thar Desert).

1 Introduction

The United Nations Intergovernmental Panel on Climate Change (IPCC) in its Fifth Assessment Report (AR5) suggests that the average global land and ocean temperature has increased by approximately 0.72 (0.49–0.89) °C during 1951–2012 with a linear trend of 0.12 (0.08–0.14) °C/decade (Guo et al. 2017; IPCC 2014). Accompanied by this increase in temperature, there was a noticeable increase in climate extremes around the world (Choudhary and Dimri 2018; Piras et al. 2016; Aslam et al. 2017; Dash and Mamgain 2011). For future climate projections, Regional Climate Models (RCMs) indicate that the frequency and intensity of climate extremes will increase due to the increase in global temperature. The intensity of yearly maximum 1-day (5-day) precipitation events will rise by 9.2% (8.5%) under the 1.5 °C WT and 12.6% (11%) under 2 °C warming target (WT) (Li et al. 2018). To avoid suffering from more severe climate extremes and limit anthropogenic influence on climate systems, world leaders during the twenty-first Conference of the Parties (COP21) meeting agreed upon to take steps towards restricting the global mean temperature rise to well below 2 °C of pre-industrial levels. They further agreed to pursue efforts towards a target of 1.5 °C (Xu et al. 2017; UNFCCC 2015).

The global WT, which is determined for the global mean temperature rise relative to the pre-industrial or base-period climatology, is the subject of recent active research. The World Meteorological Organization (WMO) states that 14 of the 15 hottest years on record have all fallen in the twenty-first century (WMO 2015). So some nations, organizations, and scientists have suggested that global mean temperature should not rise over 2 °C above pre-industrial levels. A global WT of 2 °C above pre-industrial levels has been set forth as a preliminary target by many countries, European Union, and international organizations (Hansen 2005). It is believed that if the temperature rise passes this threshold, then the climate system would undergo an irreversible dangerous change. This change could be in terms of extreme weather and climate events, depleting freshwater resources, sea level rise, negative food production, ocean acidification, biodiversity reduction, and ultimately impacts upon the human living environment (Jury et al. 2015).

✉ Mahender Choudhary
mah_thory@yahoo.co.in

Deepak Kumar Prajapat
dprajapat.dk30@gmail.com

Jyoti Lodha
lodhajyoti@gmail.com

[1] Civil Engineering Department, Malaviya National Institute of Technology Jaipur, Jaipur, India

Climate models are closest possible mathematical representation of the actual system. These are the only tools available for future climate projections and analysis (Singh and Rao 2018; Giorgi and Gao 2018). Future climate projections come with uncertainties. Several methods to analyse model performance are described in literature (Jiang et al. 2016; Pierce et al. 2009; Gleckler et al. 2008). The model performance was evaluated using correlation, root-mean-square (RMS) error, and variance ratio. These three statistics were combined in a single diagram, resulting in nice graphical visualizations of model performance (Taylor 2001; Boer and Lambert 2001). The model performance index (MPI) was used to evaluate the performance of three generation models (CMIP1, CMIP2, and CMIP3) to simulate the present-day mean climate (Reichler and Kim 2008; Jury et al. 2015). It was found that the current models are indeed not perfect, but they are much more realistic than their predecessors.

Recently, many scientific communities had conducted numerous studies on global climate change under different WTs (Li et al. 2018; Karmalkar and Bradley 2017; King and Karoly 2017; Seneviratne et al. 2016; Guiot and Cramer 2016; Klimenko et al. 2016; Steinacher et al. 2013; Ying 2012; Meinshausen et al. 2009). The objectives were to evaluate the possible greenhouse gas (GHG) emission pathways to achieve the 1.5/2 °C target or predict changes in extreme climate events under the WTs. Most previous studies were only based on the simulations from the Global Climate Models (GCMs), while fewer ones can be seen using the RCM simulations.

Trend of maximum and minimum temperature was analysed for past 102 years over India (Dash et al. 2007). The minimum temperature sharply falls in north India from 1955 to 1972 and then an equally sharp rise over the past three to four decades in the last century. It is possible that the global temperature rise could exceed 4 °C in the 2070s under A1FI scenario (Betts et al. 2011). The 2 °C WT is projected to occur in the median years 2047 and 2038 under RCP4.5 and RCP8.5, respectively while the area-averaged warming over China would exceed 5 °C under RCP8.5 scenario (Zhang et al. 2013). The 2 °C target will be reached sometime between 2040 and 2060 under SRES A2 and A1B emission scenarios projected by a multi-model ensemble of CMIP3 (Joshi et al. 2011).

Multi-model and multi-scenario temperature and precipitation projections were studied for different seasons over India based on CMIP5 model simulations of RCP2.6, RCP4.5, RCP6.0, and RCP8.5 scenarios (Chaturvedi et al. 2012). Multi-model ensembles (MME) were analysed in three time periods as the 2030s (2021–2050), 2060s (2046–2075), and 2080s (2070–2099) and found that CMIP5 multi-model ensemble mean climate is closer to observed climate than any individual model. There is a temperature rise between 1.7 and 2.02 °C by 2030s and 2 and 4.8 °C by 2080s relative to a pre-industrial period over the Indian region. Regional climate model projection under the A1B scenario analysed by Dash et al. (2012) and found that the annual mean temperature over northeast India may increase by 5 °C by the end of the twenty-first century. Extreme climate events were analysed over China with a 2 °C global warming (Lang and Sui 2013). A 2 °C global warming above pre-industrial times was identified to occur in the year 2029 (2025–2033) in the SRES A1B.

Threshold crossing time (TCT) for 2 °C WT in near-surface mean temperature was analysed using 39 GCMs (Jiang et al. 2016). It was found that under RCP4.5 scenario, 32 of 39 GCMs simulate global warming above 2 °C during 2017–2087 in the twenty-first century. Under RCP8.5, global warming crosses the 2 °C target in the years ranging from 2017 to 2058 for all 39 GCMs. Guo et al. (2016) analysed the precipitation extremes for eight global WTs by 17 CMIP5 models and MME. The TCT years simulated by MME are 2027 (2024), 2047 (2038), and 2075 (2050) when global warming attains 1.5 °C, 2.0 °C, and 2.5 °C WTs, respectively, under the RCP4.5 (RCP8.5) scenario. Warming of 1.5 °C, 2 °C, and 3 °C relative to 1901–1930 was analysed using 32 CMIP5 models and their MME under RCP4.5 and RCP8.5 for the USA (Karmalkar and Bradley 2017). They also found that ensemble mean surface air temperature is projected to reach 1.5 °C by 2030 under both RCPs whereas the 2 °C target is achieved by 2040 (2050) under RCP8.5 (RCP4.5). Warming of 3 °C was projected to reach soon after 2060 for RCP8.5, but not in the twenty-first century for RCP4.5. Xu et al. (2017) and Jiang et al. (2009) investigated precipitation and its extremes over Asia under 1.5–4 °C global WTs and found that the mean temperature over Asia increases by 2.3 °C, 3 °C, 4.6 °C, and 6 °C at global WTs of 1.5 °C, 2 °C, 3 °C, and 4 °C, respectively, relative to the pre-industrial era.

Singh and Rao (2018) analysed the uncertainties (model and internal variability) in future changes in temperature and precipitation over the homogeneous regions of India using CMIP5 datasets under the RCP8.5 scenario. They found that model uncertainty was larger for temperature than uncertainty due to internal variability in most areas. Highest uncertainties were observed over the northwest region, western Himalayas, and central northeast regions. The global drought extremes are projected to increase under 1.5 °C and 2 °C warming. The drought frequency is expected to increase by 5% (14%) at 1.5 °C (2 °C) warming in the surface soil moisture (Xu et al. 2019). The uncertainty in TCT was analysed for 2 °C WT by Chen and Zhou (2016). The ratio of intermodal standard deviation (σ) and warming rate (ρ) was defined as the uncertainty of TCT. In RCP4.5 and RCP8.5, the 2 °C TCT of annual mean SAT averaged in China is about 2033 ± 15 and 2029 ± 10, respectively, relative to the pre-industrial period (1961–1890). The uncertainty of the 2 °C TCT was observed to be larger under RCP4.5 than RCP8.5.

Towards a better insight into the TCTs and uncertainty associated with eight Indian warming targets (IWTs) (1.5–5

°C) above base-period (1951–1970) levels in the twenty-first century, we perform an analysis of nine experiments within the framework of the CORDEX-SA experiments. We evaluated the performance of RCMs to simulate the near-surface mean temperature over India. The multi-model ensemble projections of five CORDEX-SA experiments were used to analyse the spatial distribution of TCTs and its uncertainty for different IWTs under RCP4.5 and RCP8.5 scenarios. Accordingly, the structure of this paper is as follows. Section 1 describe the introduction followed by Section 2 which describes the study area and datasets used in this study. Section 2 also describes the methodology adopted in this study. Section 3 evaluates the performance of the CORDEX-South Asia project in simulating the near-surface mean temperature and further analysis of the threshold crossing time. It also has the uncertainty for eight IWTs projected by MME mean with the discussion on results. A brief conclusion is finally presented in Section 4.

2 Material and methods

India is the seventh largest country in the world with an area of 32,87,263 km^2. To understand the response of climate to the warming thresholds, the target region for analysis is selected as the whole country. Due to the extensive size and complex geography, it has large spatial and temporal variations. The Indian Institute of Tropical Meteorology (IITM), Pune, has divided the whole India into seven homogeneous temperature zones. These seven zones are north-west, western Himalaya, north-central, north-east, interior peninsula, east coast, and west coast (Chakraborty et al. 2019; Kishore et al. 2016; Madhu et al. 2015; Dash and Mamgain 2011; Dash and Hunt 2007; Dash et al. 2007; Kumar et al. 1994). These seven zones are agro-climatically and geographically distinct from each other as explained below.

The western Himalaya is cold arid ecoregion having shallow skeletal soils. This region receives significant precipitation in the form of snow during the winter months due to the movement of mid-latitude westerly synoptic systems commonly known as Western Disturbances. The average annual rainfall in this zone is 750–1500 mm. The mean summer temperature (July) varies from 5 to 30 °C and mean winter temperature ranges around − 24.1 to 6.8 °C (Negi et al. 2018). In this zone, a specific pattern of vegetation (alluvial grasslands, subtropical forest, conifer mountain forests, and alpine meadows) is found due to changes in altitude. This region also contains 50% of India's native plant species and 10% of the world's known higher-altitude plant and animal species. The mountains are 300 to 6000 m high which are natural barrier to species migration (Tewari et al. 2017; Padma and Nakul 2014).

The north-west zone is hot arid and semi-arid subtropical region. There is Great Indian Thar desert in this zone, extending over about 320 thousand km^2 area. It covers 10% of total geographic area of India (Sharma and Mehra 2009). This zone contains the desert soil, loamy saline and alkali soils. It receives annual rainfall less than 250 mm in arid region and between 250 and 750 mm in semi-arid subtropical regions. The mean summer temperature in this zone varies between 25 and 40 °C and mean winter temperature between 10 and 25 °C.

East-coast region is hot sub-humid to semi-arid ecoregion with alkaline coastal, deltaic alluvium-derived soil and loamy to clayey soil. It is a narrow shelf and wide stretch of land area with bays, estuaries, lagoons, deltas and some smaller islands and salt marsh. The width of east coast is between 100 and 130 km (Mukhopadhyay and Karisiddaiah 2014). The mean annual rainfall varies between 1000 and 3000 mm (Pramanik et al. 2015). The mean summer temperature is 28–38 °C while in winter it varies between 20 and 30 °C, coupled with high levels of humidity. The East coast region is bounded by hilly terrain known Eastern Ghats (Saha et al. 2017). The west coast is a narrow strip of land (50–100 km) sandwiched between the western Ghat and the Arabian Sea (Mukhopadhyay and Karisiddaiah 2014). It is a hot humid region having deep loamy to clayey, mixed red and black soils. The average annual rainfall in this zone is more than 2000 mm. The average temperature in July varies between 25 and 30 °C while in January it varies between 18 and 28 °C.

In the north-east zone, climate is humid subtropical with hot, humid summers, severe monsoons, and mild winters having brown and red hill soils, lateritic soil, and yellow soils. It is covering a geographical area of 26.2 mha out of 72% area under hilly ecosystems (Soraisam et al. 2018; Laskar et al. 2014). The area is characterized by rich biodiversity, heavy precipitation, and high seismicity. The average annual rainfall in this zone is more than 2000 mm. This region occupies 7.7% of the total geographical area of India and supports 50% of the flora (i.e. 8000 species), of which 31.58% is endemic. The mean July temperature varies between 25 and 35 °C while in January it varies between 10 and 25 °C.

Interior peninsula zone has humid and semi-arid tropical climate. It is roughly triangle in shape. The average height of region is 600–900 m above sea level, and some parts have over 1000-m height (Khullar 1999). The central and western peninsula has semi-arid climate while eastern peninsula has humid climate. In interior peninsula zone, annual average rainfall is 500–2000 mm. The average temperature in July is 25–40 °C, and in January it varies between 12–28 °C. This region is rich in red and black (Regur) soils. North-central zone has sub-humid continental and sub-humid transitional climatology. Average annual rainfall in this zone varies between 750 and 2000 mm. Average temperature of July varies between 25 and 40 °C while in January it varies between 10

and 25 °C (Husain 2014). This soil in this region is classified as alluvium-derived soils, deep black soils. The most significant weather events affecting India are heat waves, cold waves and fog, snowfall, floods and droughts, monsoon depressions, and cyclones. The impacts of climate change also differ from one region to the other. The methodology used for analysis is briefly described below.

2.1 Methodology

In order to find TCT for different IWTs in seven zones, data from CORDEX-SA experiments has been used. A significant bias can be generally found in the experiment's simulations when compared with the observed CRU data. Thus, a bias correction method is first implemented by observations. The Delta bias correction method is used to correct the future projections of all nine CORDEX-SA experiments. The performance of nine experiments is evaluated to simulate the parameter T_{mean} using the model performance index (MPI). After that, the TCT for eight IWTs (1.5, 2, 2.5, 3, 3.5, 4, 4.5, and 5 °C) is analysed with the projected uncertainty in TCT of IWTs.

2.1.1 Model performance index

The model performance index can be used to evaluate the skill of models to reproduce the different climate variables (Reichler and Kim 2008). It also combines the performance of multiple parameters in one index. The reason to select this method is it considers the mean bias which is an essential component of model error. Murphy et al. (2004) also used a similar approach. In this study, we use this method to evaluate the performance of the CORDEX experiment to reproduce the T_{mean}. The base period for observations was 1971–2000. To obtain MPI, in the first step normalized error variance e_m^2 is calculated for each model m (Eq. (1)). It is the total of square gridpoint differences between the modelled and observed climatology normalized by the corresponding gridpoint interannual variance.

$$e_m^2 = \sum_n \left[w_n \left(\overline{s_{mn}} - \overline{o_n} \right)^2 / \sigma_n^2 \right] \tag{1}$$

$$I_m^2 = e_m^2 / \overline{e_m^2} \tag{2}$$

In Eq. (1) $\overline{s_{mn}}$ denotes the simulated climatology of a model and $\overline{o_n}$ is the observed climatology, σ_n^2 the interannual variance, and w_n a gridpoint-specific weighting term. By normalizing the individual error variances over the ensemble mean error variances, the MPI I_m^2 is obtained that varies evenly around one (Eq. (2)). MPIs close to and smaller than one indicate models that perform better than the average; MPIs larger than one indicate the opposite. The calculation of the mean MPI over several single model runs is carried out in the same way (Jiang et al. 2016).

2.1.2 TCTs for different Indian warming targets

IWTs are the temperature thresholds (1.5, 2, 2.5, 3, 3.5, 4, 4.5, and 5 °C) which are considered for the rise in T_{mean} relative to base-period (1951–1970) climatology. TCT for an IWT is the time when projections of T_{mean} change will exceed that target above base-period levels. The TCTs are determined relative to the base-period climate to calculate the years in which the Indian T_{mean} rise would reach 1.5 °C, 2 °C, 2.5 °C, 3 °C, 3.5 °C, 4 °C, 4.5 °C, and 5 °C thresholds under the RCP4.5 and RCP8.5 scenarios. To determine the TCTs for different IWTs, the 20-year period of 1951–1970, within the longer 149-year period, is considered a base period. The 30 years of 1971–2000 is considered the present climate; the future forecasting data is generated by model simulations which are based on the representative concentration pathway (RCP) scenarios.

To reduce the uncertainty in calculating the TCT due to inter-annual variability, the T_{mean} rise was projected for a 9-year running average. In the 9 years, the median year was considered TCT when the specific IWT will cross and both the 4 years before and after the median year. To reduce uncertainties from inter-model differences, we also calculate the multi-model ensemble mean using five best performing CORDEX-SA experiments. The MME mean usually shows higher reliability to reproduce the present climate relative to an individual model. Therefore, multi-model mean with equal weights is calculated here, which has been widely used in the projection of anthropogenic climate change.

2.1.3 Analysis of projected uncertainties of TCT for IWTs

The policymakers need to understand the uncertainties in simulations and projections of future climate change in order to select appropriate adaption measures. To estimate the TCT uncertainty, two factors were proposed (Chen and Zhou 2016). These two factors are represented by the inter-modal standard deviation (σ) and warming rate (ρ) around the TCT. These two factors are used to estimate the TCT uncertainty.

The T_{mean} linear increase with time was expressed as

$$T = \rho t + T' \tag{3}$$

where, in Eq. (3), T is temperature, t is time, ρ is warming rate crossing a certain threshold T_0, and T' is the reference temperature before warming ($t = 0$). Thus, the TCT for T_0 should be $(T_0 - T')/\rho$. Further considering the T_{mean} uncertainty in different models, Eq. (3) becomes

$$T = \rho t + T' \pm \sigma \tag{4}$$

where σ is the inter-model standard deviation and assumed as a constant (Eq. (4)). Further, the TCT is derived as $\frac{T_0-T'}{\rho} \pm \frac{\sigma}{\rho}$ and the ratio of $\pm\frac{\sigma}{\rho}$ is rightly the uncertainty of TCT.

The equation for inter-model standard deviation (σ) (Guo et al. 2016; Li and Zhou 2010) can be written as

$$\sigma = \sqrt{\frac{1}{n}\sum_{i=1}^{n}\left(X_i - \overline{X}\right)^2} \tag{5}$$

In Eq. (5), X_i is the output of a single model, $\overline{X}$ is the MME output, and n is the number of models. Larger values of σ show greater uncertainty in the projection. Theil-Sen slope estimator test (Sen 1968) is used to determine the warming rate. This is a non-parametric test which has been used in several studies (Prajapat and Choudhary 2018).

2.2 CORDEX-SA experiments

Coordinated Regional Climate Downscaling Experiments (CORDEX) is a globally coordinated project under which simulations by multiple RCMs driven with different GCMs (hereafter, experiments) are carried out over different domains or regions across the world. This project was initiated to study regional climate change scenarios globally (Choudhary and Dimri 2018; Fernández et al. 2010; Giorgi et al. 2009). One such domain of interest under CORDEX is South Asia (SA), which includes the Indian subcontinent. For this study, a total nine CORDEX-SA experiments, i.e. three RCMs forced with nine GCMs in different combinations, are used, which comes from CMIP5 (refer to Table 1 for experiment names and other details) and their ensemble.

The (2 m) near-surface mean temperature (T_{mean} used interchangeably hereafter) data for India was acquired from Centre for Climate Change Research (CCCR), Indian Institute of Tropical Meteorology (IITM), Pune, India. The CCCR RCM data has spatial resolution of 0.44° (~ 50 km) at daily, monthly, or annual temporal resolution. The T_{mean} from simulations of nine experiments for 149 years (1951–2099) is analysed in the study at annual temporal scale. The study region consists of 1297 grid points. The necessary information for these experiments is listed in the Table 1. Output of each experiment is compared with the observed gridded dataset of Climate Research Unit (CRU) TS V 4.00 (1971–2000), which is also available at ~ 50 km resolution for bias correction. After bias correction, model performance has been evaluated and the best experiments were selected for further TCT and its uncertainty analysis. The results and discussion of the study are given in the following sections.

3 Results and discussion

Data from CORDEX-SA is checked for any bias, and there is a significant cold, and warm bias found in all nine experiments and multi-model ensemble (MME). A significant cold bias is found in the western Himalayan (North India) region and north-east regions. The other regions, north-west, north-central, east-coast, and west-coast, have warm bias during 1971–2000. The annual mean bias in MME projection varies from − 14.8 to 1.88 °C. Maximum cold bias is seen in CNRM (− 19.95 °C) and the maximum warm bias in CSIRO (6.31 °C) experiment. The IPSL experiment shows the minimum cold bias as − 10.79 °C, and CNRM shows minimum warm bias as 1.40 °C. So we can say that all the experiments are unable to simulate the T_{mean} correctly in the hilly regions of India. The bias correction is performed using the delta bias method. Further, the performance of all nine experiments is evaluated.

3.1 Evaluation of the performance of CORDEX-experiments to simulate mean temperature

The performance of all nine CORDEX experiments is carried out using the model performance index (MPI). The outcome of the comparison of nine experiments regarding I^2 is illustrated in the Table 2. Individual I^2 values can be used to rank the experiments. The results indicate large differences from one experiment to another regarding their ability to match the observations of present climate.

For a better performing experiment, the I^2 index should be close to and less than one. The I^2 value higher than one represents the underperforming experiment. The CanESM experiment performs best to simulate the T_{mean} over India. Table 2 shows that two models have MPI values higher than one (CNRM, GFDL) and two model have very low MPI value (IPSL, MIROC); therefore these four are not used in further analysis. Five remaining experiments that perform well to represent T_{mean} over the Indian region are used to calculate MME mean.

3.2 Spatial distribution of threshold crossing times corresponding to 1.5–5 °C warming threshold over India projected by MME

For a better insight into the timing and climate change associated with 1.5–5 °C warming above base-period levels in the twenty-first century, analysis is performed using five CORDEX experiments. Figures 1 and 2 show the spatial distribution of TCTs for 1.5–5 °C WTs over India under RCP4.5, and RCP8.5 scenarios projected by the MME mean. The geographical distribution of TCT when 1.5–5 °C warming of annual T_{mean} will reach varies with different regions in each scenario.

Table 1 Details of CORDEX-SA experiments analysed in the present study (source: CORDEX South-Asia Database, CCCR, IITM; http://cccr.tropmet.res.in/cordex/files/downloads.jsp)

S.N.	Experiment name	Name used in the study	CORDEX South Asia RCM	RCM description	Contributing CORDEX modelling centre	Driving CMIP5 GCM	Contributing CMIP5 modelling centre
1	CCCma-CanESM2- IITM-RegCM4	CanESM2	IITM-RegCM4	The Abdus Salam International Center for Theoretical Physics (ICTP) Regional Climate Model version 4 (RegCM4) (Giorgi et al. 2012)	Centre for Climate Change Research (CCCR), Indian Institute of Tropical Meteorology (IITM), India	CCCma-CanESM2	Canadian Centre for Climate Modelling and Analysis (CCCma), Canada
2	GFDL-ESM2M-IITM-RegCM4	GFDL				NOAA-GFDL-GFDL-ESM2M	National Oceanic and Atmospheric Administration (NOAA), Geophysical Fluid Dynamics Laboratory (GFDL), USA
3	IPSL-CM5A-LR-IITM-RegCM4	IPSL				IPSL-CM5A-LR	Institut Pierre-Simon Laplace (IPSL), France
4	CSIRO-Mk3.6.0-IITM-RegCM4	CSIRO				CSIRO-Mk3.6.0	Commonwealth Scientific and Industrial Research Organisation (CSIRO), Australia
5	MIROC-MIROC5-SMHI-RCA4	MIROC	SMHI-RCA4	Rossby Centre regional atmospheric model version 4 (RCA4) (Samuelsson et al. 2011)	Rossby Centre, Swedish Meteorological and Hydrological Institute (SMHI), Sweden	MIROC-MIROC5	Model for Interdisciplinary Research On Climate (MIROC), Japan Agency for Marine-Earth Sci. & Tech., Japan
6	CNRM-CM5-SMHI-RCA4	CNRM				CNRM-CM5	Centre National de Researchs Me'te' orologiques (CNRM), France
7	MOHC-HadGEM2-ES-SMHI-RCA4	HadGEM				MOHC-HadGEM2-ES	Met Office Hadley Centre (MOHC), UK
8	NCC-NorESM1-M-SMHI-RCA4	NorESM				NCC-NorESM1-M	Norwegian Climate Change, Norway
9	MPI-ESM-LR-REMO2009	MPI	MPI-CSC-REMP2009	MPI-Regional model 2009 (REMO 2009) (Teichmann et al. 2013)	Climate Service Center (CSC), Germany	MPI-ESM-LR	Max Plank Institute for MPI-M, Germany

Table 2 Model performance index I^2 for all nine experiments

S.N	Experiment name	MPI
1	CanESM	0.94
2	CSIRO	0.86
3	GFDL	2.26
4	MPI	0.60
5	CNRM	1.90
6	IPSL	0.40
7	MIROC	0.57
8	HadGEM	0.80
9	NorESM	0.61

3.2.1 Spatial distribution of TCTs for IWTs under RCP4.5

Figure 1 represents the spatial distribution of TCTs for different IWTs under the RCP4.5 scenario. The results show that up to 3.5 °C warming will occur under RCP4.5 in the twenty-first century.

The 1.5 °C TCT of T_{mean} across India varies from 2014 to 2056 under the RCP4.5 scenario. Warming of 1.5 °C first occurs in North India (western Himalaya) during 2014–2025 and after that in north-west, north-central and interior peninsula regions during 2025–2040. After that, it is registered in the north-east, east-coast, and west-coast of India during 2040–2056. An average 1.5 °C TCT is 2034. The warming in the entire study area will cross the 1.5 °C WT, and the TCT for most of the area is before 2035. The 1.5 °C warming rate is faster in western Himalaya and relatively slow in north-east India. At present, the time when 2 °C warming of annual T_{mean} would occur has been of wider concern. Figure 1 represents that the patterns of occurrence of all WTs are common (as similar to 1.5 °C WT) for all WTs. The TCT for 2 °C WT varies from 2022 to 2079 (average TCT 2047) and will occur in 99.62% area of India. Few grids in East-coast of India do not represent the warming of 2 °C in the twenty-first century.

The TCT for 2.5 °C WT varies in the period of 2036 to 2086 (average TCT 2066). In the twenty-first century, warming will cross 2.5 °C WT in 85.04% of the area in India. The 14.96% area of India does not represent the warming of 2.5 °C or above in the twenty-first century that includes most of East-coast, west-coast regions, and some regions of the north-east. The TCT for 3 °C WT varies from 2044 to 2086. Only 28.29% of the area in India represent the warming of 3 °C. These areas are western Himalayan and north-western India. in the western Himalayan region, the TCT for 3 °C varies from 2044 to 2075, while in the north-western region the TCT for 3 °C is around 2080. An average TCT for 3 °C WT is 2072. The TCT for 3.5 °C WT varies from 2058 to 2091. The warming of 3.5 °C is found mostly in the western Himalayan region. In India, the warming will cross 3.5 °C WT in 7.01% area in the twenty-first century. An average TCT for 3.5 °C WT is 2073.

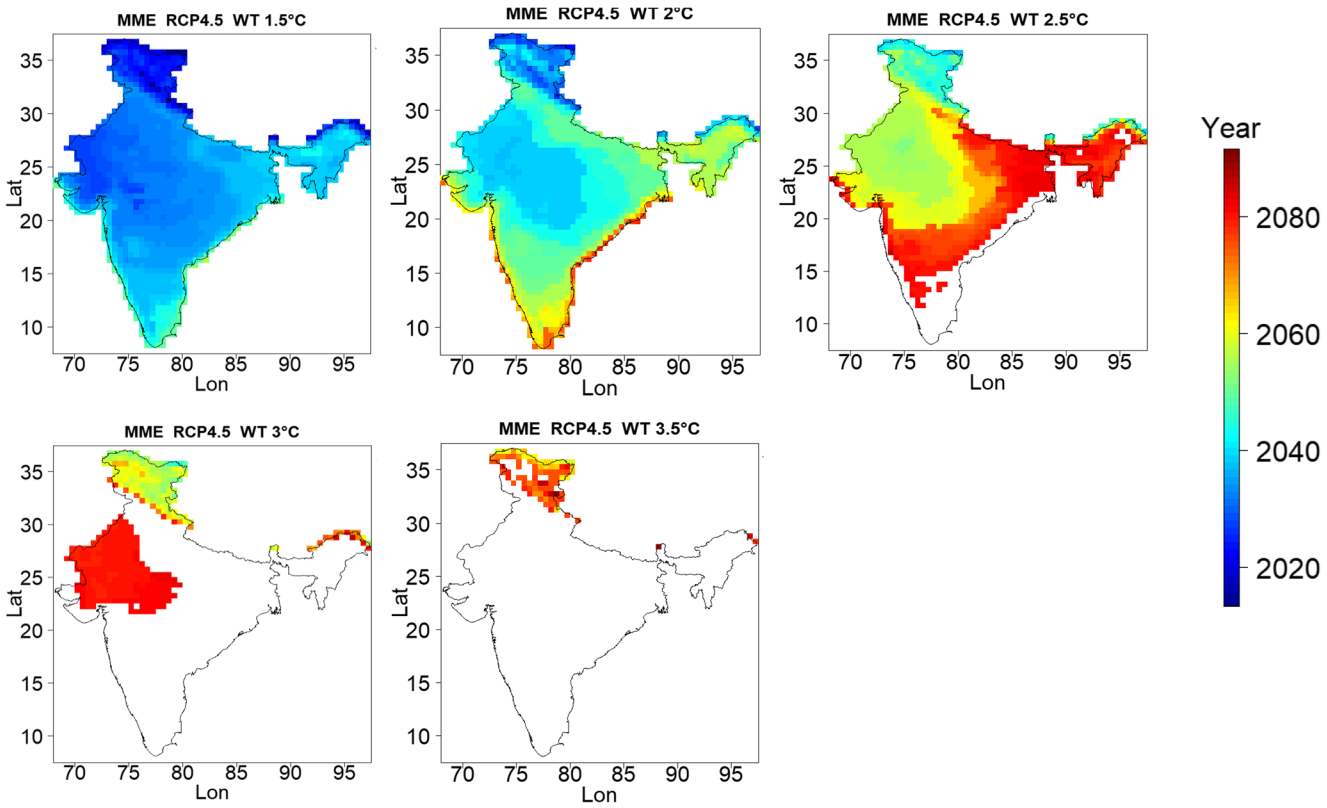

Fig. 1 Spatial distribution of TCTs for different Indian warming targets (IWTs) under the RCP4.5 scenario

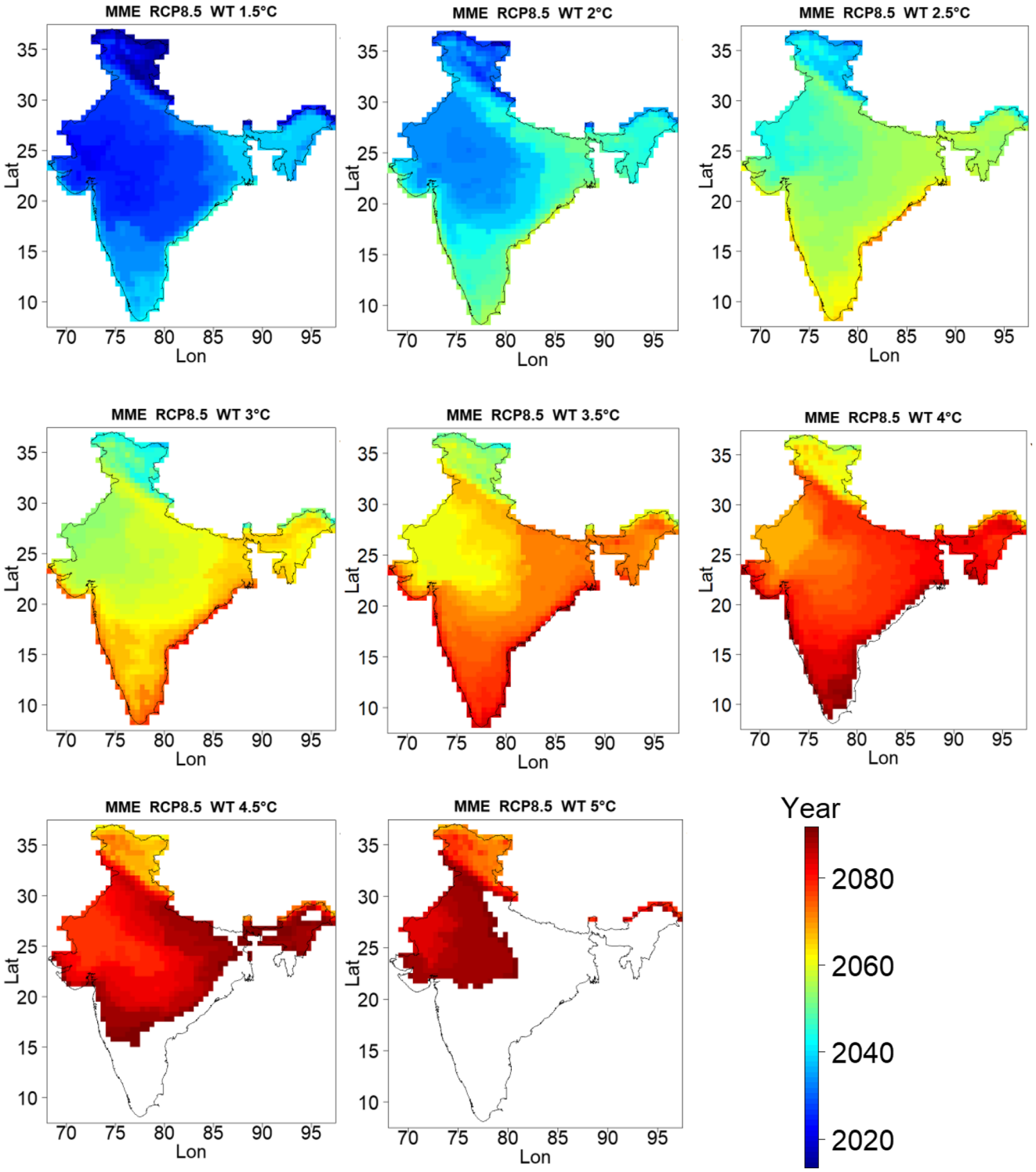

Fig. 2 Spatial distribution of TCTs for Indian warming targets (IWTs) under the RCP8.5 scenario

3.2.2 Spatial distribution of TCTs for IWTs under RCP8.5

Spatial distribution of TCTs projected by MME simulations for different IWTs under the RCP8.5 scenario is shown in Fig. 2. The results show that all eight IWTs will occur under RCP8.5. The spatial distribution of TCTs represents that the TCT for 1.5 °C WT varies from 2014 to 2047. The spatial distribution of TCT shows that the 1.5 °C WT will occur initially in the western Himalayan region (2014–2025) followed by some regions of north-west, north-central, and interior

peninsula (2025–2035). In the east-coast, west-coast, and north-east India 1.5 °C warming will occur in mid-century (2035–2047). So we found that the warming of 1.5 °C will occur earlier in the western Himalaya and north-west of India and later in north-east India. The entire study region will get the warming of 1.5 °C before the mid-twenty-first century. The average TCT for 1.5 °C WT is 2030 which is 4 years earlier than TCT under RCP4.5. The TCT for 2 °C WT varies from 2018 to 2060. The average TCT for 2 °C WT is 2041 which is 6 years earlier than TCT under RCP4.5. The entire study area will get the warming of 2 °C before 2060. Figure 2 represents that the spatial occurrence patterns of all WTs are similar to each other and only the time of occurrence and area vary for all WTs. The 2.5 °C warming TCT varies from 2030 to 2072. The average TCT for 2.5 °C WT is 2053 which is 13 years earlier than TCT under RCP4.5. The entire study area will get the warming of 2.5 °C before 2072. The 3 °C WT in India will occur during the period of 2037–2082. The average TCT for 3 °C WT is 2061 which is 11 years earlier than TCT under RCP4.5. The entire study area will get the warming of 3 °C before 2082.

The TCT for 3.5 °C WT spatially varies from 2044 to 2091. The average TCT for 3.5 °C WT is 2069 which is only 4 years earlier than TCT under RCP4.5. The 99.62% study area will get the warming of 3.5 °C under RCP8.5. Some grids in the east-coast region do not represent the warming of 3.5 °C in the twenty-first century. The TCT for 4 °C WT varies from 2053 to 2091. The 4 °C WT will occur in 95.14% of area. Some grids in the East-coast and west-coast regions do not represent the warming of 4 °C or above in the twenty-first century. The average TCT for 4 °C WT is 2077. The TCT for 4.5 °C WT varies from 2061 to 2091. An average TCT for 4.5 °C WT is 2082. The 75.32% study area will get the warming of 4.5 °C under RCP8.5. The TCT for 5 °C WT varies from 2067 to 2091. In the 37.93% area of India, the warming will cross the 5 °C WT. These areas are western Himalayan (2067–2085) and north-west (2086–2091) of India. The upper region of north-east India also represents warming of 5 °C during 2080–2085. An average TCT for 5 °C WT is 2085.

3.3 Projection of 1.5–5 °C warming for whole India by regionally averaged MME T_{mean}

The annual average T_{mean} will continue to rise in India. RCP4.5 is a medium stabilization scenario that stabilizes radiative forcing at 4.5 W m^{-2} in the twenty-first century without ever exceeding that value. Under global warming, it is interesting to take the whole of India as one and then investigate how its T_{mean} would evolve over time. A regionally average time series is created for T_{mean} anomaly relative to the base-period (1951–1970) period and TCT, its uncertainty is evaluated. The average T_{mean} of India in base period was 22.55 °C. Under this pathway, all five best performing experiments represent the warming of 1.5 °C and 2 °C, while only 4 experiments show warming of 2.5 °C, and only 2 experiments forecast warming of 3 °C in the twenty-first century. None of the experiments shows the warming above 3 °C target by the twenty-first century under RCP4.5. RCP8.5 is the pathway with the highest greenhouse gas emissions, and hence the largest radiative forcing by the end of this century. The rise in average T_{mean} is more substantial in this scenario than RCP4.5. In this scenario, projections of all five experiments represent the warming up to 3.5 °C, and 4 experiments show the warming of 4 °C and 4.5 °C, but only 2 experiments represent the warming of 5 °C in the twenty-first century.

The threshold crossing times for different IWTs are shown in Fig. 3 under (a) RCP4.5 and (b) RCP8.5 for five best performing CORDEX-SA experiments and their multi-model ensemble (MME). The dotted black line represents the warming targets and their threshold crossing time for MME.

The threshold crossing time projected by MME for 1.5 °C WT is 2033 (ranging from 2030–2043 for all five experiments) and 2028 (ranging from 2023–2033) under RCP4.5 and RCP8.5 respectively. The threshold crossing time for 2 °C warming is 2044 (2043–2070) and 2039 (2035–2047) for RCP4.5 and RCP8.5 respectively. The multi-model ensemble simulation for whole India indicates that the warming in RCP4.5 (RCP8.5) scenario does not cross the 2.5 °C (4.5

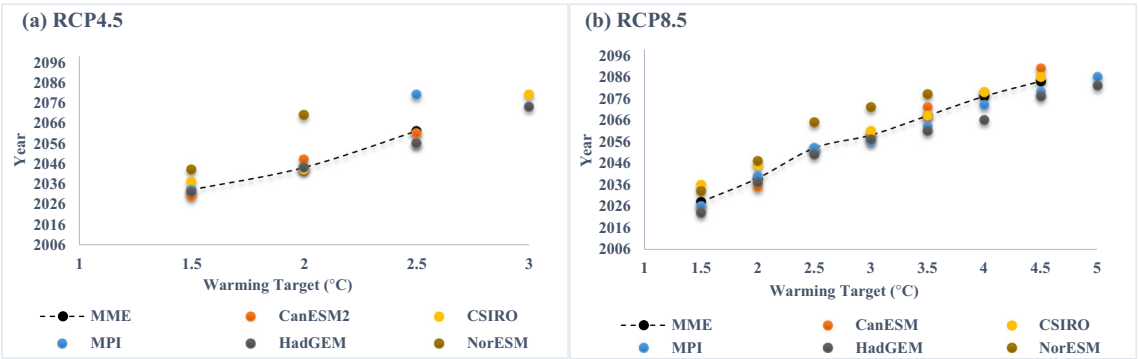

Fig. 3 Threshold crossing time projected by five COREDEX experiments and multi-model ensemble (MME) for eight IWTs (1.5, 2.0, 2.5, 3.0, 3.5, 4.0, 4.5, and 5.0 °C) under **a** RCP4.5 scenarios and **b** RCP8.5 scenario

Table 3 Threshold crossing times (TCTs) for different IWTs projected by the multi-model ensemble (MME) and corresponding uncertainty range, temperature uncertainty (σ), and warming rate (ρ) near the TCT and their ratio (σ/ρ) in India under RCP4.5 and RCP8.5

Scenarios	Indian warming target	TCT (uncertainty range)	σ (°C)	ρ (°C/10a)	σ/ρ (10a)
RCP4.5	1.5 °C	2033 (2032, 2035)	0.11	0.40	0.27
	2 °C	2044 (2038, 2050)	0.19	0.29	0.65
	2.5	2062 (2050, 2090)	0.34	0.18	1.8
RCP8.5	1.5 °C	2028 (2025, 2029)	0.11	0.43	0.25
	2 °C	2039 (2036, 2042)	0.10	0.40	0.25
	2.5 °C	2053 (2050, 2055)	0.22	0.65	0.33
	3 °C	2059 (2055, 2064)	0.30	0.60	0.50
	3.5 °C	2068 (2062, 2073)	0.36	0.58	0.62
	4 °C	2077 (2071, 2083)	0.40	0.62	0.64
	4.5 °C	2084 (2077, 2091)	0.45	0.59	0.76

°C) WT in the twenty-first century. The threshold crossing time (TCT) for 2.5 °C, 3 °C, 3.5 °C, 4 °C, and 4.5 °C WTs are 2053, 2059, 2068, 2077, and 2084, respectively, under RCP8.5 indicated by MME simulation.

3.4 Analysis of projected uncertainties in TCT for IWTs projected by MME

Due to high uncertainty in future climate simulation, it is important to quantify the uncertainties in threshold crossing time projected by five CORDEX-SA experiments under two RCPs. To understand the uncertainties in TCT for all IWTs, we examined the average T_{mean} in the twenty-first century.

3.4.1 Controlling factors of TCT uncertainty

Based on the Eq. (4), σ and ρ are two main factors determining TCT uncertainty. Here we represent how σ and ρ play their roles in the different TCTs in two (RCP4.5 and RCP8.5) scenarios. The value of σ and ρ around TCT of all WTs were determined, and their ratio σ/ρ was calculated (Table 3) for all India T_{mean} projected by MME. The intermodal standard deviation was high for 1.5 °C WT and low for 2 °C and 2.5 °C WT in RCP8.5 than RCP4.5. The results revealed that the intermodal standard deviation is high for higher WTs. The warming rate (ρ) calculated from Sen's slope estimator test is converted into warming rate per decade. As the RCP8.5 is higher emission scenario, so the warming rate for all WTs is higher in this scenario than RCP4.5. For 1.5 °C WT the warming rate is higher than other WTs under RCP4.5. Under RCP8.5 the warming rate is almost similar for 1.5–2 °C WT (0.43 and 0.40 °C/10a) and 2.5–4.5 °C WTs (0.58–0.65 °C/10a). The ratio of σ/ρ for 1.5 °C TCT is 0.27 and 0.25 under RCP4.5 and RCP8.5. For 2 °C and 2.5 °C σ/ρ is larger in RCP4.5 (0.65 and 1.8) than RCP8.5 (0.25 and 0.33). This is mainly caused by the higher warming rate and lower intermodal standard deviation under RCP8.5 as compared with RCP4.5. It was found that the uncertainty in TCT increases from lower to higher WTs under both RCPs.

σ is the 21-year average of intermodal standard deviation around the TCT; 10a is decade; ρ is 21-year linear trend of mean temperature around the TCT

3.4.2 Characteristics of TCT uncertainty

Table 3 also represents the TCT for different IWTs projected by MME and their corresponding uncertainty range. The average T_{mean} uncertainty and warming rate near TCT and their ratio are also represented for different IWTs of RCP4.5 and RCP8.5 scenarios.

The 1.5 °C TCT of average T_{mean} in India is about 2033 ± 3 and 2028 ± 3 in RCP4.5 and RCP8.5 scenarios, respectively. The 2 °C TCT of average T_{mean} in India is about 2044 ± 7 and 2039 ± 3 in RCP4.5 and RCP8.5 scenarios, respectively. The warming above 2.5 °C WT was not found under RCP4.5, while under RCP8.5 the average T_{mean} will cross the 4.5 °C WT. The TCT and their uncertainty for 2.5 °C, 3 °C, 3.5 °C, 4 °C, and 4.5 °C are 2053 ± 4, 2059 ± 5, 2068 ± 7, 2077 ± 7, and 2084 ± 8 under RCP8.5. The uncertainty range of WTs is expressed as the range of time when average T_{mean} anomalies varying between ± 1σ (intermodal standard deviation) to reach the WT. The uncertainty range calculated by ± 1σ is found larger in RCP4.5 than RCP8.5. The uncertainty range in TCT is higher for high WTs. The uncertainty calculated by σ/ρ ratio is well represented by the uncertainty range.

The study represents the performance of CORDEX experiments to simulate T_{mean} and spatial distribution of TCT for eight IWTs. Northern India and north-west regions are preeminent regions of India. North Indian region contains the great Himalayan region while in the north-west region, there is the Great Indian Desert (Thar). The climate conditions in both regions are entirely different from each other and ecologically sensitive. Our results are supported by other studies carried out over India (Singh and Rao 2018). All models show a clear signal of gradually wide-spread warming throughout the

twenty-first century. There is maximum rapid warming seen in the western Himalayan region (Hilly regions) followed by north-west (Thar Desert) region.

4 Conclusions

In this study, the performance of nine CORDEX-SA experiments to simulate the T_{mean} is carried out using the model performance index (MPI). The spatiotemporal distribution of TCT for eight IWTs relative to base-period (1951–1970) levels is projected using MME of the five best performing CORDEX-SA experiments over India. The TCT and its uncertainty are also investigated using projections of MME. The primary conclusions are as follows.

- The model performance index shows that T_{mean} over the Indian region is best represented by five CORDEX-SA experiments, namely CanESM, CSIRO, HadGEM, NorESM, and MPI. So, for analysis of IWT projected by multi-model ensemble (MME), these five models were used. The CanESM experiment performs best to simulate the T_{mean} over India.
- Analysis of all India average T_{mean} of MME represents that for RCP4.5 and RCP8.5 scenarios, 1.5 °C TCT is 2033 ± 3 and 2028 ± 3 respectively. The spatial distribution of TCTs by MME projections represents that five IWTs (1.5–3.5 °C) will occur in the twenty-first century under RCP4.5. The TCT for 1.5 °C WT across India varies from 2014 to 2056 under the RCP4.5 scenario. All eight IWTs will occur in the twenty-first century under RCP8.5. The average TCT for 1.5 °C WTs is 2030 under RCP8.5 which is 4 years earlier than TCT under RCP4.5 scenario.
- The spatial distribution of TCT projected by MME represents that warming will cross the 3 °C WT over entire India in the twenty-first century under RCP8.5. Under RCP4.5, 2 °C WT will occur almost in entire India.
- The results revealed that the intermodal standard deviation (σ) is high for higher WTs under both RCPs. Under RCP8.5 the warming rate (ρ) is almost similar for 1.5 and 2 °C WT and 2.5 to 4.5 °C WTs. For 2 °C, and 2.5 °C IWT the uncertainty (σ/ρ) is larger in RCP4.5 than RCP8.5. This is mainly caused by higher warming rate and lower intermodal standard deviation under RCP8.5 as compared with RCP4.5. It is found that the uncertainty in TCT increases from lower to higher WTs under both RCPs.

Acknowledgements We acknowledge the World Climate Research Programme's Working Group on Regional Climate, the Working Group on Coupled Modelling which formerly coordinated CORDEX. The authors also thank the Earth System Grid Federation (ESGF) infrastructure and the Climate Data Portal at Centre for Climate Change Research (CCCR), Indian Institute of Tropical Meteorology, India, for provision of CORDEX-SA data.

Compliance with ethical standards

Conflict of interest The authors declare that they have no conflict of interest.

References

Aslam AQ, Ahmad SR, Ahmad I, Hussain Y, Hussain MS (2017) Vulnerability and impact assessment of extreme climatic event: a case study of southern Punjab, Pakistan. Science of the Total Environment 580:468–481

Betts RA, Collins M, Hemming DL, Jones CD, Lowe JA, Sanderson MG (2011) When could global warming reach 4 C? Philosophical Transactions of the Royal Society A: Mathematical, Physical and Engineering Sciences 369(1934):67–84

Boer GJ, Lambert SJ (2001) Second-order space-time climate difference statistics. Climate Dynamics 17(2-3):213–218

Chakraborty R, Venkat Ratnam M, Basha SG (2019) Long-term trends of instability and associated parameters over the Indian region obtained using a radiosonde network. Atmospheric Chemistry and Physics 19(6):3687–3705

Chaturvedi RK, Joshi J, Jayaraman M, Bala G, Ravindranath NH (2012) Multi-model climate change projections for India under representative concentration pathways. Current Science 103(7):791–802

Chen X, Zhou T (2016) Uncertainty in crossing time of 2°C warming threshold over China. Science bulletin 61(18):1451–1459

Choudhary A, Dimri AP (2018) Assessment of CORDEX-South Asia experiments for monsoonal precipitation over Himalayan region for future climate. Climate Dynamics 50(7-8):3009–3030

Dash SK, Hunt JC (2007) Variability of climate change in India. Current Science 93(6):782–788

Dash SK, Mamgain A (2011) Changes in the frequency of different categories of temperature extremes in India. Journal of Applied Meteorology and Climatology 50(9):1842–1858

Dash SK, Jenamani RK, Kalsi SR, Panda SK (2007) Some evidence of climate change in twentieth-century India. Climatic change 85(3-4): 299–321

Dash SK, Sharma N, Pattnayak KC, Gao XJ, Shi Y (2012) Temperature and precipitation changes in the north-east India and their future projections. Global and Planetary Change 98:31–44

Fernández J, Fita L, Garcia-Diez M et al (2010) WRF sensitivity simulations on the CORDEX African domain. In EGU General Assembly Conference Abstracts (Vol. 12, p. 9701)

Giorgi F, Gao XJ (2018) Regional earth system modeling: review and future directions. Atmospheric and Oceanic Science Letters 11(2): 189–197

Giorgi F, Jones C, Asrar GR (2009) Addressing climate information needs at the regional level: the CORDEX framework. World Meteorological Organization (WMO) Bulletin 58(3):175

Giorgi F, Coppola E, Solmon F, Mariotti L, Sylla MB, Bi X, Elguindi N, Diro GT, Nair V, Giuliani G, Turuncoglu UU (2012) RegCM4: model description and preliminary tests over multiple CORDEX domains. Climate Research 52:7–29

Gleckler PJ, Taylor KE, Doutriaux C (2008) Performance metrics for climate models. Journal of Geophysical Research: Atmospheres 113(D6)

Guiot J, Cramer W (2016) Climate change: The 2015 Paris Agreement thresholds and Mediterranean basin ecosystems. Science 354(6311): 465–468

Guo X, Huang J, Luo Y, Zhao Z, Xu Y (2016) Projection of precipitation extremes for eight global warming targets by 17 CMIP5 models. Natural Hazards 84(3):2299–2319

Guo X, Huang J, Luo Y, Zhao Z, Xu Y (2017) Projection of heat waves over China for eight different global warming targets using 12 CMIP5 models. Theoretical and applied climatology 128(3-4): 507–522

Hansen JE (2005) A slippery slope: how much global warming constitutes "dangerous anthropogenic interference?". Climatic Change 68(3):269–279

Husain M (2014) Geography of India. Tata McGraw-Hill Education, India

IPCC, Climate Change (2014) Synthesis Report. Cambridge University Press, Cambridge and New York

Jiang D, Lang X, Sui Y (2009) Ensemble projection of 1–3°C warming in China. Chinese Science Bulletin 54(18):3326–3334

Jiang D, Sui Y, Lang X (2016) Timing and associated climate change of a 2°C global warming. International Journal of Climatology 36(14): 4512–4522

Joshi M, Hawkins E, Sutton R, Lowe J, Frame D (2011) Projections of when temperature change will exceed 2°C above pre-industrial levels. Nature Climate Change 1(8):407–412

Jury MW, Prein AF, Truhetz H, Gobiet A (2015) Evaluation of CMIP5 models in the context of dynamical downscaling over Europe. Journal of Climate 28(14):5575–5582

Karmalkar AV, Bradley RS (2017) Consequences of global warming of 1.5°C and 2°C for regional temperature and precipitation changes in the contiguous United States. PLoS One 12(1):e0168697

Khullar DR (1999) India: A comprehensive geography. Kalyani Publishers, India

King AD, Karoly DJ (2017) Climate extremes in Europe at 1.5 and 2 degrees of global warming. Environmental Research Letters 12(11): 114031

Kishore P, Jyothi S, Basha G, Rao SV, Rajeevan M, Velicogna I, Sutterley TC (2016) Precipitation climatology over India: validation with observations and reanalysis datasets and spatial trends. Climate dynamic 46(1-2):541–556

Klimenko VV, Klimenko AV, Mikushina OV, Tereshin AG (2016) To avoid global warming by 2°C—mission impossible. Thermal Engineering 63(9):605–610

Kumar KR, Kumar KK, Pant GB (1994) Diurnal asymmetry of surface temperature trends over India. Geophysical Research Letters 21(8): 677–680

Lang X, Sui Y (2013) Changes in mean and extreme climates over China with a 2°C global warming. Chinese Science Bulletin 58(12):1453–1461

Laskar SI, Kotal SD, Roy Bhowmik SK (2014) Analysis of rainfall and temperature trends of selected stations over North East India during last century. Mausam 65(4):497–508

Li B, Zhou TJ (2010) Projected climate change over China under SRES A1B scenario: multi-model ensemble and uncertainties. Adv. Clim. Change Res 6(4):270–276

Li H, Chen H, Wang H, Yu E (2018) Future precipitation changes over China under 1.5° C and 2.0°C global warming targets by using CORDEX regional climate models. Science of The Total Environment 640:543–554

Madhu S, Kumar TL, Barbosa H, Rao KK, Bhaskar VV (2015) Trend analysis of evapotranspiration and its response to droughts over India. Theoretical and applied climatology 121(1-2):41–51

Meinshausen M, Meinshausen N, Hare W, Raper SC, Frieler K, Knutti R, Frame DJ, Allen MR (2009) Greenhouse-gas emission targets for limiting global warming to 2 °C. Nature 458(7242):1158–1162

Mukhopadhyay R, Karisiddaiah SM (2014) The Indian coastline: processes and landforms. In Landscapes and landforms of India:91–101

Murphy JM, Sexton DM, Barnett DN, Jones GS, Webb MJ, Collins M, Stainforth DA (2004) Quantification of modelling uncertainties in a large ensemble of climate change simulations. Nature 430(7001): 768–772

Negi HS, Kanda N, Shekhar MS, Ganju A (2018) Recent wintertime climatic variability over the north west Himalayan cryosphere. Current Science 114(4):760–770

Padma TV, Nakul C (2014) Himalayan plants seek cooler climes. Nature News 512(7515):359

Pierce DW, Barnett TP, Santer BD, Gleckler PJ (2009) Selecting global climate models for regional climate change studies. Proceedings of the National Academy of Sciences U.S.A. 106(21):8441–8446. https://doi.org/10.1073/pnas.0900094106

Piras M, Mascaro G, Deidda R, Vivoni ER (2016) Impacts of climate change on precipitation and discharge extremes through the use of statistical downscaling approaches in a Mediterranean basin. Science of the Total Environment 543:952–964

Prajapat DK, Choudhary M (2018) Spatial distribution of precipitation extremes over Rajasthan using CORDEX data. ISH Journal of Hydraulic Engineering 4:1–2

Pramanik MK, Biswas SS, Mukherjee T, Roy AK, Pal R, Mondal B (2015) Sea level rise and coastal vulnerability along the eastern coast of India through geospatial technologies. J. Remote Sens. GIS 4: 2469–4134. https://doi.org/10.4172/2469-4134.1000145

Reichler T, Kim J (2008) How well do coupled models simulate today's climate? Bulletin of the American Meteorological Society 89(3): 303–312

Saha U, Chakraborty R, Maitra A, Singh AK (2017) East-west coastal asymmetry in the summertime near surface wind speed and its projected change in future climate over the Indian region. Global and Planetary Change 152:76–87

Samuelsson P, Jones CG, Willén U, Ullerstig A, Gollvik S, Hansson UL, Jansson E, Kjellström MC, Nikulin G, Wyser K (2011) The Rossby Centre Regional Climate model RCA3: model description and performance. Tellus A: Dynamic Meteorology and Oceanography 63(1):4–23

Sen PK (1968) Estimates of the regression coefficient based on Kendall's tau. Journal of the American statistical association 63(324):1379–1389

Seneviratne SI, Donat MG, Pitman AJ, Knutti R, Wilby RL (2016) Allowable CO_2 emissions based on regional and impact-related climate targets. Nature 529(7587):477–483

Sharma KK, Mehra SP (2009) The Thar of Rajasthan (India): ecology and conservation of a desert ecosystem. In Faunal ecology and conservation of the Great Indian Desert 2009 (pp. 1-11). Springer, Berlin, Heidelberg. https://doi.org/10.1007/978-3-540-87409-6_1

Singh R, Rao AK (2018) Quantifying uncertainty in twenty-first century climate change over India. Climate Dynamics:1–24

Soraisam B, Karumuri A, Pai DS (2018) Uncertainties in observations and climate projections for the North East India. Global and Planetary Change 160:96–108

Steinacher M, Joos F, Stocker TF (2013) Allowable carbon emissions lowered by multiple climate targets. Nature 499(7457):197–201

Taylor KE (2001) Summarizing multiple aspects of model performance in a single diagram. Journal of Geophysical Research: Atmospheres 106(D7):7183–7192

Teichmann C, Eggert B, Elizalde A, Haensler A, Jacob D, Kumar P, Moseley C, Pfeifer S, Rechid D, Remedio A, Ries H (2013) How does a regional climate model modify the projected climate change signal of the driving GCM: a study over different CORDEX regions using REMO. Atmosphere 4(2):214–236

Tewari VP, Verma RK, Gadow KV (2017) Climate change effects in the Western Himalayan ecosystems of India: evidence and strategies. Forest Ecosystems 4(1):13

UNFCCC (2015) Adoption of the Paris agreement. United Nations Office at Geneva, Geneva

World Meteorological Organization (2015) WMO Statement on the status of the global climate in 2014. World Meteorological Organization, Geneva WMO-No. 115

Xu Y, Zhou BT, Wu J, Han ZY, Zhang YX, Wu J (2017) Asian climate change under 1.5–4° C warming targets. Advances in Climate Change Research 8(2):99–107

Xu L, Chen N, Zhang X (2019) Global drought trends under 1.5 and 2° C warming. International Journal of Climatology 39(4):2375–2385

Ying Z (2012) Projections of 2.0 C warming over the globe and China under RCP4.5. Atmospheric and Oceanic Science Letters 5(6):514–520

Zhang L, Ding YH, Wu TW, Xin XG, Zhang YW, Xu Y (2013) The 21st century annual mean surface air temperature change and the 2°C warming threshold over the globe and China as projected by the CMIP5 models. Acta Meteorol Sin 71(6):1047–1060